

See discussions, stats, and author profiles for this publication at: <https://www.researchgate.net/publication/282761693>

The effect of particulate strengthening on microstructure and mechanical characterization of binary-modified composites on mild steel

Article in *Journal of Composite Materials* · September 2015

DOI: 10.1177/0021998314552002

CITATIONS

3

READS

85

3 authors:



Ojo Sunday Isaac Fayomi

Covenant University Ota Ogun State, Nigeria

173 PUBLICATIONS 585 CITATIONS

[SEE PROFILE](#)



Patricia Popoola

Tshwane University of Technology

308 PUBLICATIONS 1,452 CITATIONS

[SEE PROFILE](#)



Cleophas Loto

Covenant University Ota Ogun State, Nigeria

184 PUBLICATIONS 1,375 CITATIONS

[SEE PROFILE](#)

Some of the authors of this publication are also working on these related projects:



Upcoming International Conference on Engineering for a Sustainable World [View project](#)



Austempered Ductile Iron [View project](#)



The effect of particulate strengthening on microstructure and mechanical characterization of binary-modified composites on mild steel

OSI Fayomi^{1,2}, API Popoola¹ and CA Loto^{1,2}

Abstract

This article presents the microstructure, tribological behavior, and hardness properties of the Zn-TiO₂ functional composite coating produced using electrolytic co-deposition technique. The 7.0–13.0 weight fractions of Ti particles were incorporated in a Zn bath to form Zn-TiO₂ alloy in the presence of other additives. The microstructural properties of the fabricated coating were investigated using a scanning electron microscope equipped with an energy-dispersive spectroscope, X-ray diffraction, and an atomic force microscope. The anticorrosion behavior in 3.65% NaCl medium was studied using potentiodynamic polarization technique and characterized using high-resolution optical microscope. The hardness and wear properties of the coated alloys were measured with high diamond microhardness tester and reciprocating sliding tester, respectively. From the results, the increases in hardness and wear resistance are attributed to the formation of the incorporated particulate and uniform precipitation of the metal grains at the metal lattice. The contribution of TiO₂ particles especially with Zn-13Ti-0.3 V-S provides new orientation of metal–matrix-modified coated structure and decrease in friction coefficient. The anticorrosion resistance characteristics were found to improve significantly in response to concentration of additive.

Keywords

Particulate strengthening, mechanical properties, metal–matrix composite, corrosion

Introduction

Because of low durability, limited corrosion improvement, and average strength of zinc coating, metal–matrix composites (MMCs) and ceramic–matrix composites have emerged as accomplished materials with extensive applications in structural, aerospace, automotive, electronic, thermal, and wear industries.^{1–9} Structural modification has become an essential step to enhance the properties of the base metals with the help of several deposition techniques to give protection against wear deformation and electrochemical degradation.

Composite co-deposition with electroplating method is a prolific technique that co-deposits metallic particles through electrolyte formulation. Previously published literature^{7–13} has shown metallic deposition of oxide particles like ZnO, TiO₂, Al₂O₃, Fe₂O₃, Cr₂O₃, SiO₂, ZrO₂, and ThO₂ by composite coating technique to produce enhancing functional and

mechanical characteristics for coatings. These particulates also provide corrosion, hardness, and wear resistance. Although wear resistance is an essential property in deposition, their wear property is often attested to be difficult due to thin film.^{14–17} There are substantial reports on TiO₂ composite particles with major focus on the corrosion properties and morphological behavior and not on their mechanical properties.^{12–21} According to previous studies,^{12–15} microstructural modification is intensely affected by the volume

¹Department of Chemical, Metallurgical and Materials Engineering, Tshwane University of Technology, South Africa

²Department of Mechanical Engineering, Covenant University, Nigeria

Corresponding author:

OSI Fayomi, Department of Chemical, Metallurgical and Materials Engineering, Tshwane University of Technology, PMB X680, Pretoria, South Africa.

Email: ojosundayfayomi3@gmail.com

weight fraction of incorporated particle in the bath and the kind of particulate induced in the deposits. The admixed composite are known to impact resilient behavior on the physical, mechanical and corrosion properties through proper bath control system. The choice of weight fraction of the incorporated particle in relation to optimum bath constituent becomes paramount in coating technology and this study is not an exemption. Previous studies on zinc based had proved that composite incorporated in fraction between 2 and 10 g/l could significantly influence the coating characteristics positively and something lead to excessive agglomeration and loss of sacrificial properties.^{14,18,19}

Therefore the objective of this study is to examine the concentration effect of nanoparticle strengthened Zn-TiO₂ (Zn-Ti) from sulfate bath and to investigate its microstructural and mechanical properties, with emphases on hardness and wear trend since roles of composite in engineering and manufacturing processes are highly in demand.

Experimental procedure

Preparation of substrates

Commercially obtained mild steel (40 mm × 20 mm × 1 mm) was used as cathode substrate and 99.5% zinc plate (50 mm × 20 mm × 2 mm) were prepared as anodes. The surface preparation was performed with different grade of emery paper, as described in our previous studies.^{11,14} The sample were properly cleaned with sodium carbonate, pickled,

and activated with 10% HCl at ambient temperature for 10 s and this was followed by instant rinsing in deionized water. Table 1 shows the spectrometric chemical analysis of the mild steel substrate used in this study.

Material composition and formation

Zn-Ti composite coating was produced in a single cell containing two zinc anode and single cathode electrodes, as shown in Figure 1. The distance between the anode and the cathode is 15 mm. All chemicals used are of analytical grade and de-ionized water was used in all solutions. The formulated bath was pre-heated at 40°C with stirring at 200 r/min. The processed parameter and bath composition used in this study are shown in Tables 2 and 3. The choice of the deposition parameter is in line with the preliminary study and our previous studies.^{1,2}

The electrodes were connected to the direct current via a rectifier at varying applied potential and current density between 0.3 and 0.5 V at 2 A/cm² for 20 min. The plating was done and rinsed in distilled water; samples were air-dried and thereafter sectioned for characterization.

Table 1. Chemical composition of mild steel (wt%).

Element	C	Mn	Si	P	S	Al	Ni	Fe
Composition	0.15	0.45	0.18	0.01	0.031	0.005	0.008	Balance

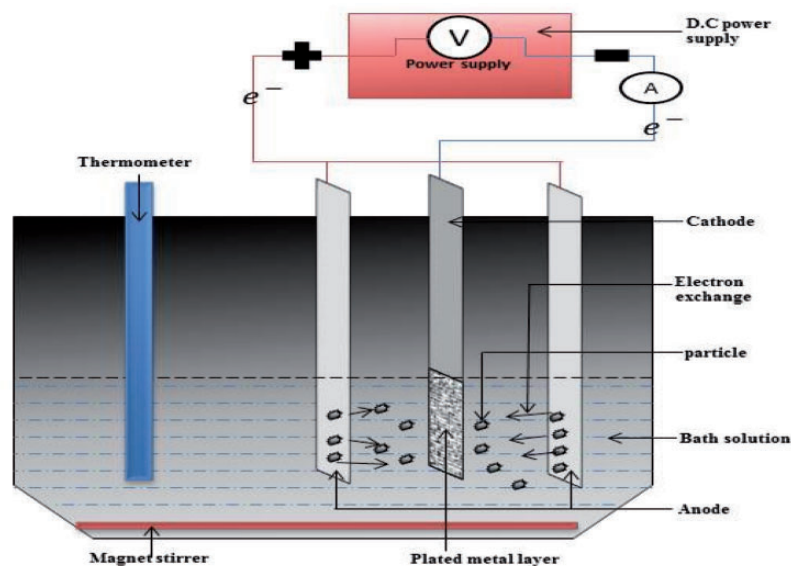


Figure 1. Schematic diagram of electrolytic deposition.

Characterization of coatings

The composite coatings obtained were characterized using a scanning electron microscopy (SEM; VEGA3 TESCAN) equipped with an energy-dispersive spectroscope. The phase change was verified using X-ray diffraction. Microhardness studies were carried out using a diamond dura-scan pyramid microhardness indenter

at a load of 10 g for 20 s. The microhardness trend was measured across the plated surface at a specific interval.

Friction and wear tests

The tribological properties of the deposited binary alloy fabricated were measured using CERT UMT-2 multifunctional tribological tester at ambient temperature of 25°C, as shown in Figure 2. The reciprocating sliding tests was carried out with a load of 5 N at constant speed of 5 mm/s and displacement amplitude of 2 mm in 20 min. A Si₃N₄ ball (4 mm in diameter, HV50 g1600) was chosen as counter body for the evaluation of tribological behavior of the coated sample. The dimension of the wear specimen was 2 × 1.5 cm. After the wear test, the structure of the wear scar and film worn tracks were further examined using Nikon optical microscope (OPM).

Table 2. Processed parameter for Zn-TiO₂ sulfate bath formulation.

Composition	Values
Zn (g/l)	75
K ₂ SO ₄ (g/l)	50
Boric acid (g/l)	10
TiO ₂ (g/l)	7–13
ZnSO ₄ (g/l)	75
pH	4.8
Voltage (V)	0.3–0.5
Time (min)	20
Temperature (°C)	40
Glycine and thiourea (g/l)	10

Electrochemical test

Autolab PGSTAT 101 Metrohm potentiostat with a three-electrode cell assembly in 3.65% NaCl static solution at 40°C was used to examine the anticorrosion studies of the composite coatings. The developed

Table 3. Electrodeposition parameters and results for Zn-TiO₂ coatings.

Sample number	Time (min)	Coating thickness (μm)	Weight gain (g)	Coating per unit area (mg/mm ²)	Voltage (V)	Additive concentration (g)
1. Zn-Ti-S	20	159.0	0.3036	0.0361284	0.3	7
2. Zn-Ti-S	20	118.0	0.1762	0.0209678	0.5	7
3. Zn-Ti-S	20	179.0	0.5398	0.0642362	0.3	13
4. Zn-Ti-S	20	264.3	0.7097	0.0768543	0.5	13

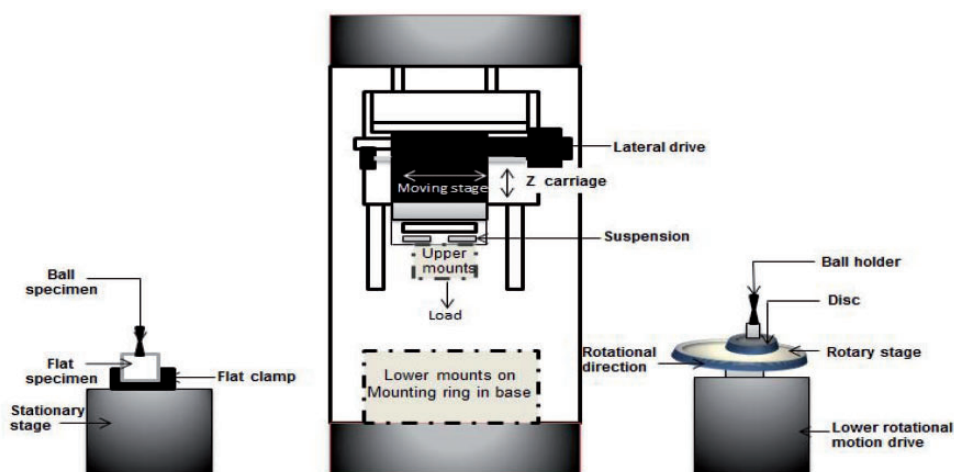


Figure 2. CERT UMT-2 reciprocating sliding friction tester.

coatings was the working electrode, platinum electrode was used as counter electrode, and Ag/AgCl was used as reference electrode. The anodic and cathodic polarization curves were recorded at a constant scan rate of 0.012 V/s, which was fixed from ± 1.5 mV.

Results and discussion

Effect of process parameters on fabricated coatings

The coatings results developed for different grade matrix of Zn-Ti sulfate depositions with their different parameters, coating thickness, weight gain, and coating per unit area, are shown in Table 3. The initial weight of the samples was measured using weighing balance with an accuracy of 0.01 g. The difference in weight obtained before and after the test shows the weight gain of the sample.

The experiments were conducted as per the summarized processed parameters and design shown in Table 2. The effect of % volume fraction (Vf %) of TiO₂ particle powder in the bath solution resulted into coating physical properties (weight gain, coating thickness and coating per unit area) presented in

Figure 3. The composite particulate could be seen to correspondently dependent on the potential. The correlation between the effects of the additive (7 and 13 g wt%) on the applied potential was quite different with both exhibiting dissimilar characteristics against incorporated composites. It is interesting to mention that at lower applied potential, the coating thickness of Zn-7Ti-0.3 V-S increases with 159 μ m compare to Zn-7Ti-0.5V-S alloy with 118 μ m for Zn-7Ti matrix. This trend does not follow the progression when the weight fraction volume was increased to 13 g wt%; at higher composite impregnation and increased maximum voltage, higher coating thickness from 179 to 264.3 μ m was attained. This characteristics is often observed in coating manufacturing because the incorporation particulate in conditioning bath have capacity to influence the throwing voltage and cause essential surface modification.

Microstructural studies

Figure 3(a) and (b) present microstructure of deposited Zn-Ti composite coatings produce at different potentials. The microstructure of Zn-7Ti-S-0.3 V (Figure 3a) was observed to contain more nucleation sites as

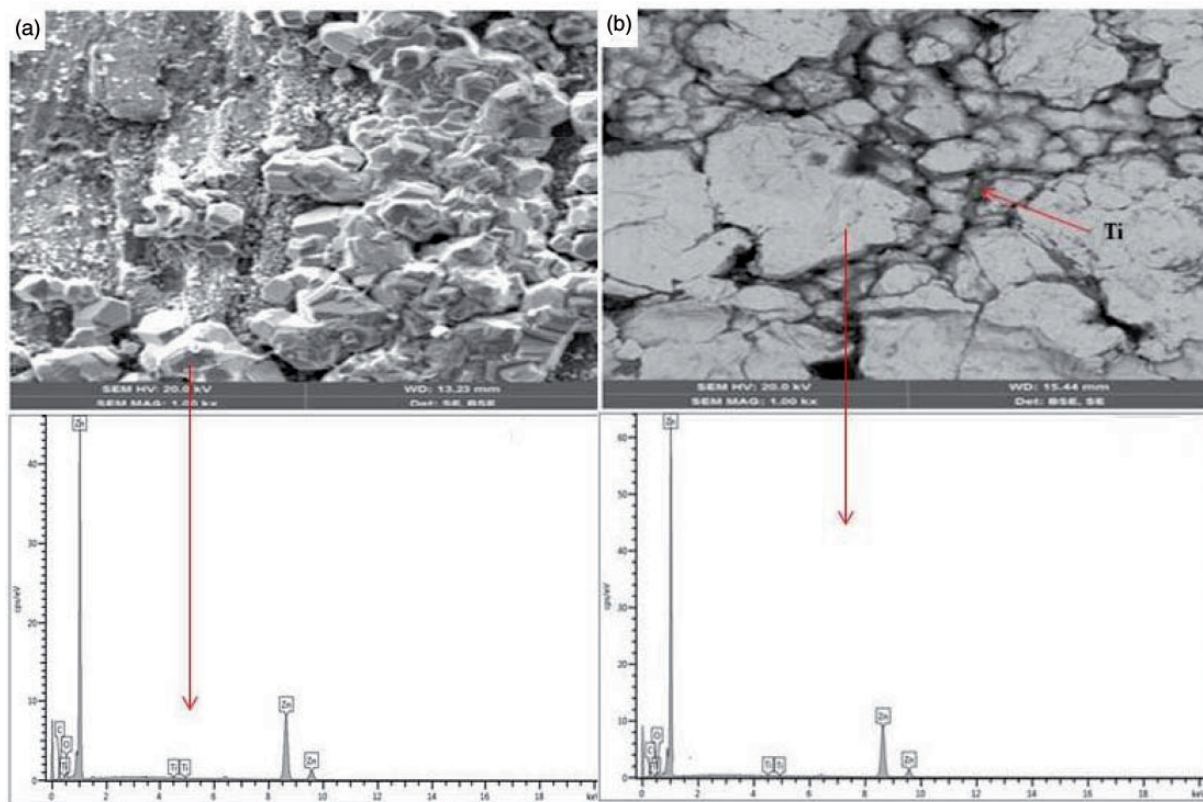


Figure 3. SEM/EDS microstructure of Zn-Ti sulfates composite deposited sample: (a) Zn-7Ti-0.3 V-S and (b) Zn-13Ti-0.3 V-S.

a result of TiO_2 interference in the zinc growth. There seems to be less uniform distribution of grain as a result of retard crystal growth. The limitation for composite embedded within the total interface could be that the incorporation of the composite-reinforced particle in deposited film absolutely depends on the plating parameter, especially the applied potential, current density, pH, and activities of the particulates.¹³ With Zn-7Ti-S-0.3 V coatings (see Figure 3b) produced at lower potential, a compactable structure was seen at the interface with porosity-free crystal.

For Zn-13Ti-0.3 V-S coating a continuous interlaced was formed, which was in line with deposited system, as shown in the study by Fayomi et al.¹⁴ In general, the formation of Ti composite on Zn precipitate was evident in Figure 3(b) with uniformity in morphology, relieve of porosity, and no stress initiation. The ability to overcome these defects is attributed to the bonding strength between the composite particles and the Zn-based alloy, which resulted to close inter-pack interface. It is important to reiterate that the mechanism for Zn-13Ti-0.3 V-S coatings entails two essential factors in relation to noble metal matrix entrapment, as reported by Su and Kao.²⁰

SEM/EDS: scanning electron microscope coupled with energy-dispersive spectroscope.

First, the agitation that is associated with the potential used during deposition and second, the adsorption of TiO_2 particle as a result of nucleation site, which favors homogeneous crystal growth of the coatings. The effect of variation of the composite particles on the Zn-Ti matrix was also examined with the help of OPM, as shown in Figure 4.

The distribution of the particles at the interface follows the morphologies of the results obtained earlier, attested by SEM studies. In general, both coatings demonstrate good morphological properties in terms of orientation and lustrous characteristics. Few pores

were found with coatings with lower fraction concentration of additives.

Atomic force microstructural studies

The various microstructures developed for different grades of fabricated Zn-Ti alloy in the electrodeposited matrix are shown in Figures 5 and 6 using an atomic force microscope (AFM). Topography of the metal composites shows difference adhesion and coating propagation within the matrices. For Zn-7Ti-S-0.3 V composite coatings, intermetallic particles have a fibrous structure and coarse-grained formation having nonuniform crystal size. The nonuniform characteristic might be due to the irregularity in the film thickness as a result of the surface roughness from bath parameter.

However, for Zn-13Ti-0.3 V-S composite alloy, high refinement of crystal growth and uniform arrangement of the distributed crystals was achieved more in Figure 6. The topographical trend of the composites was attributed to higher absorbing capacity of the reinforced particulate and formidable interfacial bound between Zn^{2+} and Ti^{2+} on the based substrate.¹⁴ Although the phenomena of adhesion is proportional to the process parameter and fraction of composite, TiO_2 is seen to exhibit less built up growth with Zn-13Ti-0.3 V-S alloy; however, good structural modification was obtained, as shown in studies of Praveen and Venkatesha³ and Shibli et al.⁷

X-ray diffraction studies

X-ray diffractograms of the composite coatings matrix at 7 and 13 g wt% fraction in 0.3 V are shown in Figures 7 and 8, respectively. The diffractogram gives major diffraction peak at 37.5° , 45° , 55° , 70° , and 77° for Zn-7Ti-S-0.3 V composite alloy, as shown in

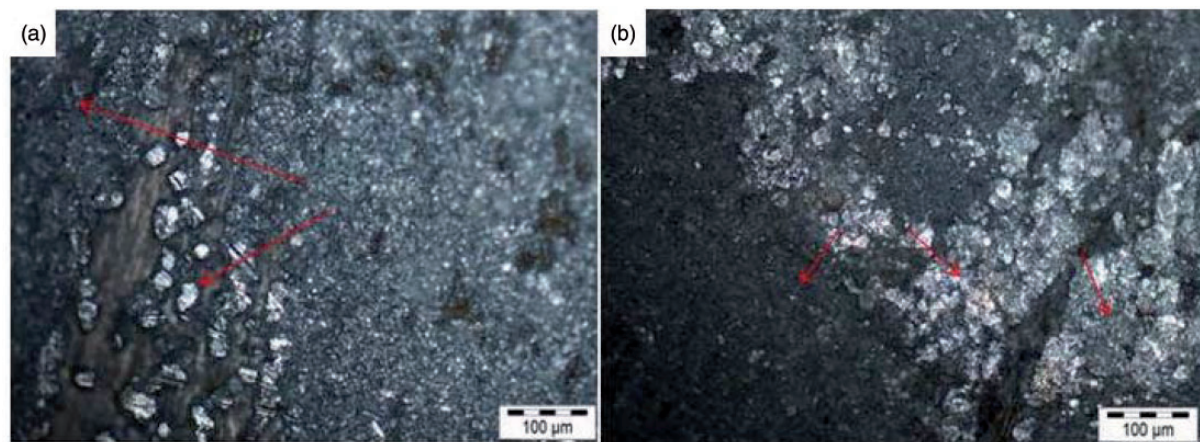


Figure 4. Morphology for Zn-Ti sulfates deposited mild steel: (a) Zn-7Ti-0.3 V-S and (b) Zn-13Ti-0.3 V-S.

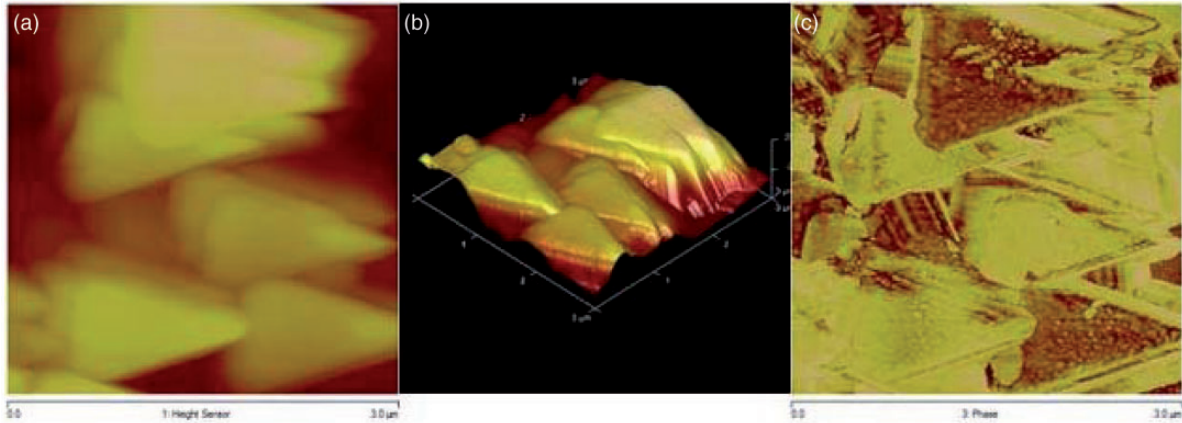


Figure 5. AFM images of the Zn-7Ti-S-0.3 V film obtained for: (a) two-dimensional image, (b) three-dimensional relief image and (c) roughness analysis.

AFM: atomic force microscope.

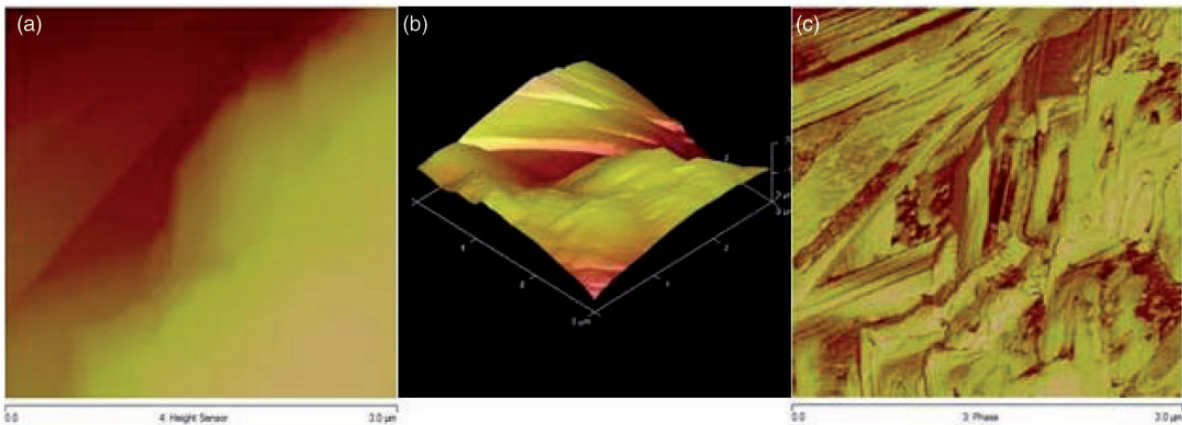


Figure 6. AFM images of the Zn-13Ti-0.3 V-S film obtained for: (a) two-dimensional image, (b) three-dimensional relief image and (c) roughness analysis.

AFM: atomic force microscope.

Figure 7. The complete mineralogical phase constitute revealed the presence of TiO_2 as a minor constituent all through the phases. The interfacial reactions with zinc identify solid composition like ZnO , $\text{Zn}_3\text{O}_7\cdot\text{Ti}$, $\text{Ti}_2\text{O}_3\cdot\text{Zn}$, TiZn , and $\text{TiZn}_3\text{O}_{12}$. Obviously, Zn particulates seem to have major dominance in some regions, which is expected because of ratio of zinc addition in the bath to other interference particles. The addition of TiO_2 particle affects not only the precipitation but also the quantity of the resultant phases. However, for Zn-13Ti-0.3 V-S alloy, some of the phases shows significantly improved peaks but at same Bragg angle position for Zn-7Ti-S-0.3 V (see Figure 8). The interaction effect of the variables and composite fraction could be seen as quiet a significant factor for the production of the peak level. Reported authors in literatures shows that significant differences in the peak level determine coatings bonding effect. The similarities in

their patterns confirmed the presence of Ti particle deposits while the differences in their peaks could be the result of the rate of deposition potential and the degree of incorporation, which is in line with the Raman studies, as shown in Figure 9.

Microhardness properties

Figure 10 shows the microhardness value (HVN) of the Zn-Ti sulfates composite coating deposits at varied applied potentials and incorporated (wt%) fraction. From the results of the Zn-Ti coatings, an appreciable increase in the hardness was observed with suitable improvement for all the composite coatings against the as-received sample.

Among the fabricated coating, Zn-7Ti-S-0.3 V possessed lower hardness quality with 85.8 HVN but showed better properties preferred when compare

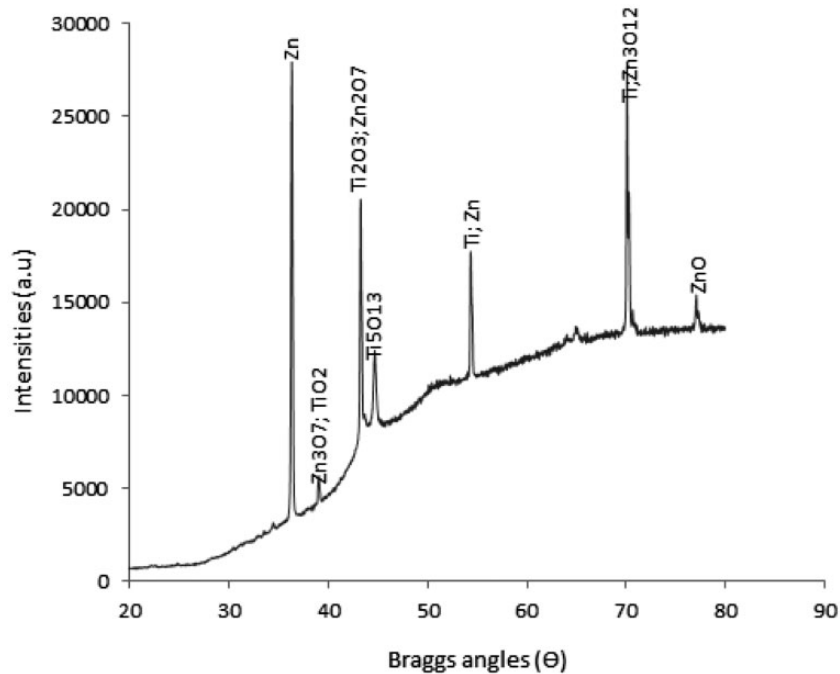


Figure 7. Solid X-ray diffraction for Zn-7Ti-0.3 V.

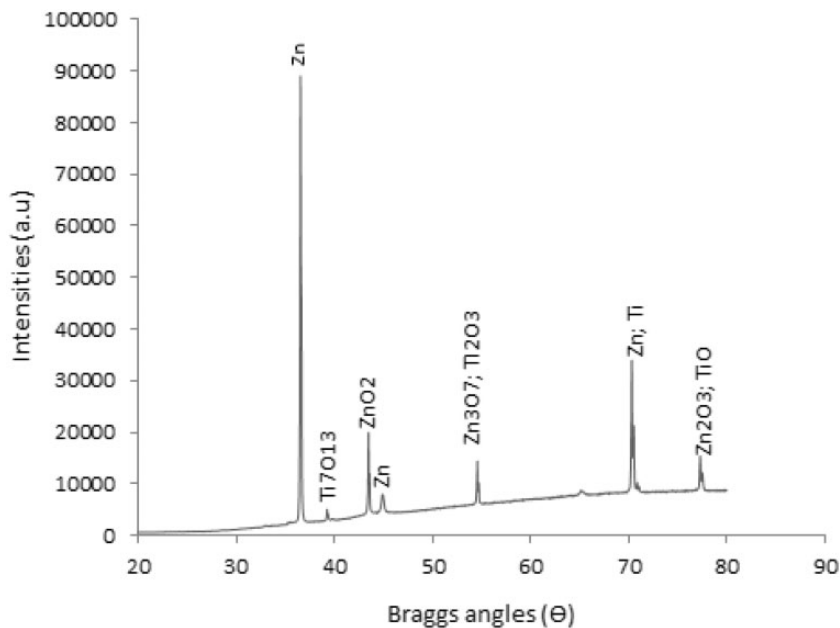


Figure 8. Solid X-ray diffraction for Zn-13Ti-0.3 V-S.

with the as-received sample with 33.5 HVN. It is anticipated that the behavior of this coating, as mentioned earlier, is the result of the degree of solid metal grain absorption on the steel interface and strong adhesion of the surface film. A coating with poor adhesion will typically show failure and retard hardenability.^{11,21} This situation is in line with the property exhibited with Zn-7Ti-S-0.3 V matrix produced. However, a significant

transition with improved hardness properties was achieved for Zn-13Ti-0.3 V-S alloy with approximately 154.5 HVN. This is good justification for the inclusion of TiO_2 particles in Zn-based matrix. This improvement in our study is on par with composite coating produced in other studies.^{1,6}

In addition, from previous literature it is affirmed that there are factors responsible for the increase in

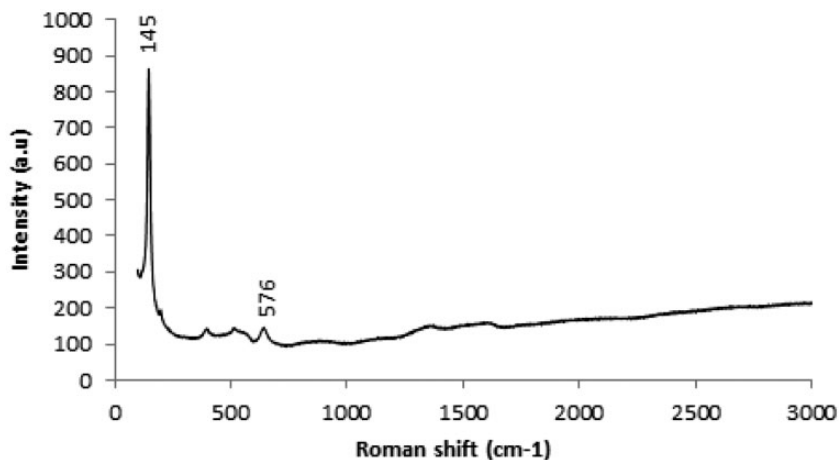


Figure 9. Raman spectral plot for Zn-13Ti-0.3 V-S sulfates deposited.

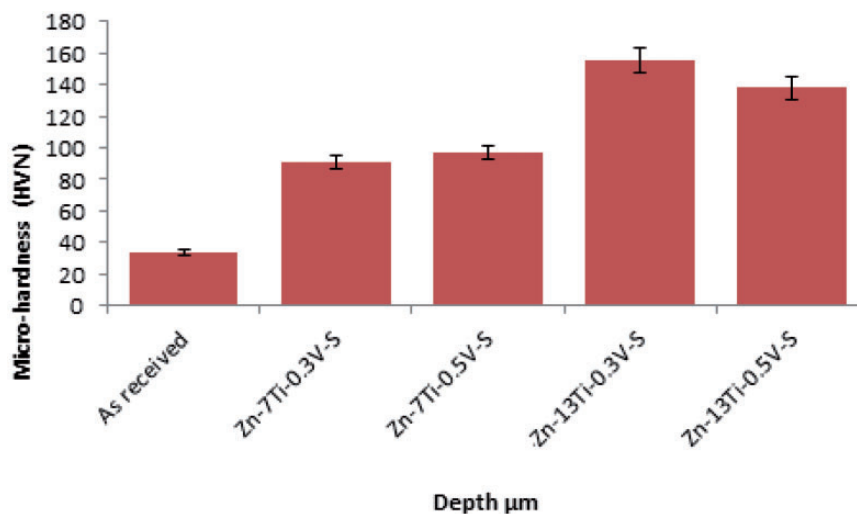


Figure 10. The microhardness/depth profile for Zn-Ti sulfates coatings.

hardness of a composite coatings, which include test conditions for the produced alloy, better bounding characteristics, and the composition and structure of the composite coating.^{4,17} In view of this, it is evident that crystallite quality and reduction in stress could influence hardness properties. With increase of TiO₂ composite particle in zinc blend, the microstructure of the composite thin film was compact; hence, the hardness resistance increased.

Wear rate evaluation

The results obtained for the wear rate study of the composite coating matrices and the as-received samples are shown in Figure 11. From the results, it can be seen that there were drastic appreciable reductions in the wear

loss for all composite alloy produced. For instance, for the most improved coating, Zn-13Ti-0.3 V-S, there was reduction of 0.006 g/min compared with the unresistible plastic deformation of 2.351 g/min for the as-received metal. At lower induced composite reinforcement of 7 g wt% in 0.3 V, the coating also retarded significantly, with reduction of 0.007 g. This implies that a suitable level of TiO₂, Metal matrix composite (MMC) incorporated in Zn-rich has been shown to improve tribological properties. The beneficial effect of the induced composite particle on the antiwear properties were best observed with low potential at higher composite reinforcement. However, it necessary to mention that it is a well known fact that the improved wear characteristic involves plastic flow, low coating wear depth, low coefficient of friction, and low

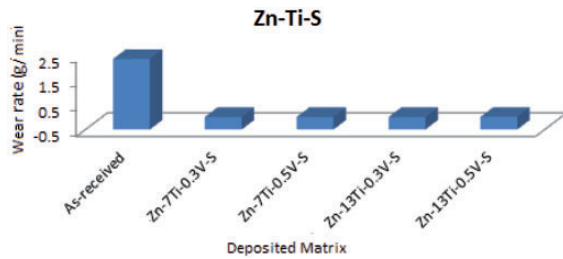


Figure 11. Variation of the wear rate with time of Zn-Ti sulfates alloy.

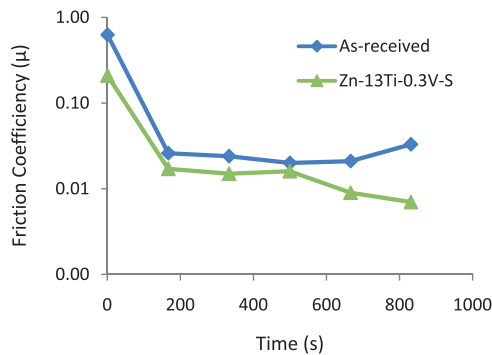


Figure 12. Variation of wear friction coefficient with time for Zn-13Ti-0.3V-S coating.

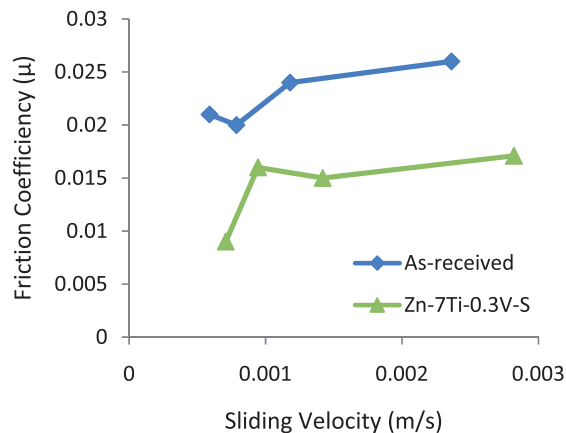


Figure 13. Variation of wear friction coefficient with sliding velocity for Zn-13Ti-0.3V-S coating.

fracture.^{9,21} Therefore, the observed decrease in wear rate is attributed to the weight percentage fraction of the composite in the bath and the structural close pack formation resulting from strong bound layer, which literally reduced the pull out and sustained adhesion.

Figures 12 and 13 present the average friction coefficient of Zn-Ti with consideration on the best composite coating (Zn-13Ti-0.3V-S) alloy and as-received samples. As can be seen, the frictional coefficient at first decreases sharply from 0.21 to 0.071 before a

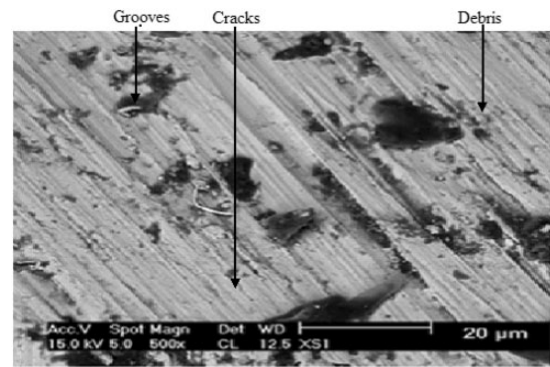


Figure 14. SEM images of the wear scar of mild steel. SEM: scanning electron microscope.

continuous slight flow toward the sliding end. In general, the coating performed excellently well having possessed lower friction coefficient against the substrate with 0.65 values under the same sliding condition. The phenomena behind this significant characteristic is attributed to the microstructure evolution, which is in line with the fact reported by Wang et al.⁶ that lower friction coefficient occurs as a result of reduction in size and quantity of particle. On the other hand, a steady flow of the sliding velocity with lower friction coefficient for deposited coating was found, as seen in Figure 13. The behavior of the as-received substrate was obvious with friction coefficient increasing as the sliding velocity increased, which ultimately tends to cause wear loss and fracture within the interface.

From the wear scar, massive degree of plastic deformation, grooves, pits, and fracture was seen on the surface of the as-received sample, as shown in Figure 14.

To compare the wear scar characteristics among the considered composite coated sample at various voltage; it was found that the wear resistance improved for Zn-13Ti-0.3V-S matrix; which can link to the effect of the new found microstructural evolutions (see Figure 15b). This was expected since lower frictional properties were attained and Wang et al.⁶ affirmed that the friction coefficient of films is depended mainly on the microstructure. Another important feature indicative of the improved antiwear properties is that the width of the wear scar is smaller, meaning that the smaller interfacial contact region between the film and the counter body causes lower friction coefficient and improved microstructure. In other word, factor responsible for the wear scar resistance could be attributed to the effect of composite particle content at moderate rate. This seems to unite with the zinc matrix to produce a uniform cluster and drastically resist the formation of micro-ploughs and film perforation, which is also in line with earlier observations by Yu et al.¹⁷ on composite

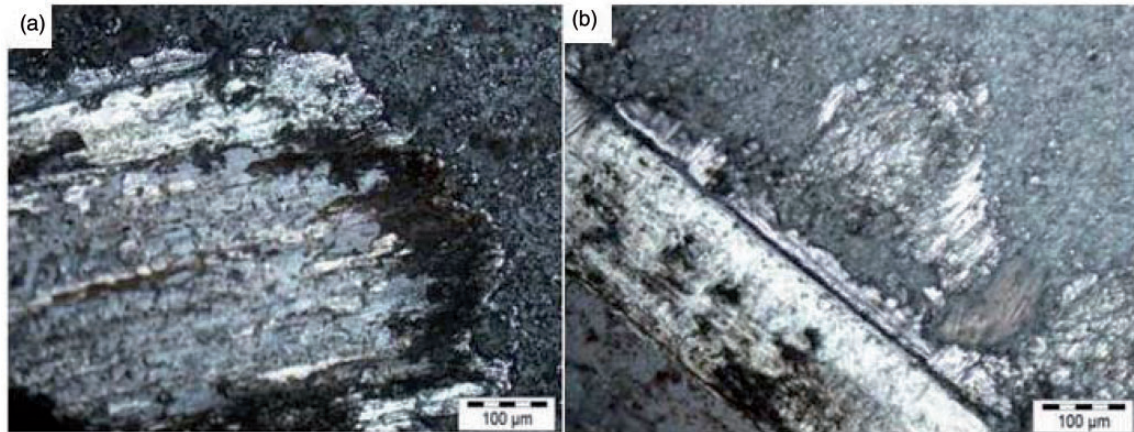


Figure 15. Wear scar of Zn-TiO₂ sulfate composites coatings: (a) Zn-7Ti-0.3 V-S and (b) Zn-13Ti-0.3 V-S.

Table 4. Summary of the potentiodynamic polarization results of Zn-TiO₂.

Sample number	I_{corr} (A/cm ²)	R_p (Ω)	E_{corr} (V)	CR (mm/year)
As received	7.04×10^{-2}	27.600	-1.53900	4.100000
Zn-7Ti-0.3 V-S	3.77×10^{-5}	291.30	-1.17035	0.015744
Zn-7Ti-0.5 V-S	2.30×10^{-5}	338.89	-1.08337	0.009586
Zn-13Ti-0.3 V-S	6.41×10^{-6}	730.61	-1.06781	0.007443
Zn-13Ti-0.5 V-S	2.24×10^{-5}	539.56	-1.06812	0.009350

deposition. When comparing these results with those of Zn-7Ti-0.3 V-S samples in Figure 15(a), few debris and pin hole were observed along the wear track, although adhesion between the composite deposit and the steel was noticed to be slightly weak with film particle dispatch as the counter pack progresses. In agreement with the reports of Gençğa et al.¹⁶ that the formation of oxide films on the wear surfaces of alloys could provide a good wear resistance, TiO₂ as hard composite to form Zn-Ti hard coating has been observed to have contributed to reduced wear ploughs on macroscale. It should be noted that stable adhesion of Zn-13Ti-0.3 V-S has a better flow than the visible irregular degradation of the former.

Electrochemical performance studies

The corrosion properties of the Zn-Ti sulfates composite coatings were observed in 3.65% NaCl in an attempt to verify the degradation and oxidation resistance mechanism with different fabricated coatings. The potential was observed to shift toward positive region for all the samples except for the substrate that moves drastically toward the more negative site. The negative potential shift of the substrate showed strong

dissolution of the mild steel films due to the absence of protection. The positive potentials shift of the as-coated samples indicates the formation of protective film and an increase in the passive film thickness. From all indications, Zn-13Ti-0.3 V-S tends to form more stable passivity than the other composite coatings due to solid incorporation of the particulate into the lattice site thereby forming a solid bound and resisting penetration of Cl⁻ ion. The results of linear tafel assessment for the various composite matrices investigated are summarized in Table 4. The corrosion potential of composite alloy with Zn-13Ti-0.3 V-S matrix is -1.06781 V while that of mild steel is -1.539 V. The lowest of the alloy matrix possess corrosion potential of -1.17035 V with an improved difference of approximately 0.369 V. This implies that reinforcement of TiO₂ in zinc interposed is beneficial to the corrosion resistance propagation even at lower volume fraction. Additionally, deposited samples displayed greatly reduced corrosion current in all instances as compared with the mild steel.

From the polarization results, mild steel had a corrosion current of 7.04×10^{-2} A/cm² as against all deposited samples. Zn-13Ti-0.3 V-S matrix have a corresponding I_{corr} value of 3.5×10^{-7} A cm⁻², which is significantly lower by five order magnitudes over mild steel. With coating fabricated with induced matrix of 7 g wt%, i.e. Zn-7Ti-0.3 V-S matrix, the corrosion density is 3.77×10^{-5} V, which show a three order improvement over the unprotected steel. Polarization resistance (R_p) for Zn-13Ti-0.3 V-S is 730.61 Ω, which was the highest attained for all composite coated samples. Three order increase in magnitude was attained when compared with 2.76×10^2 Ω for as-received sample. From the polarization behavior in Figure 16, the corrosion resistance of mild steel is enhanced drastically by the combined effort of oxide of titanium composite and Zn blend, which impose active barriers against surface susceptibility.

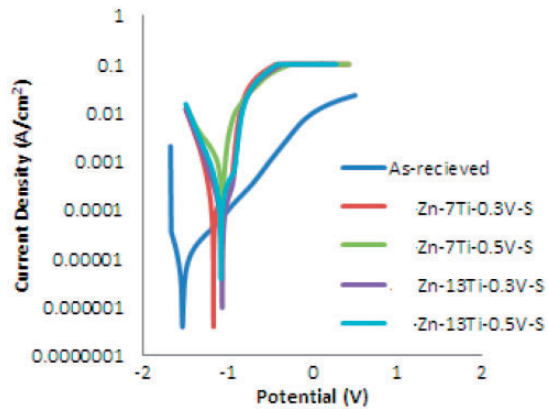


Figure 16. Linear polarization resistance (LPR) curves for Zn- TiO_2 sulfates coatings

To assess the degree of damage and the passivation on the composites coatings after corrosion studies, Figures 17 and 18 show the photomicrographs of Zn-13Ti-0.3V-S matrix obtained using AFM and OPM. The coating surface shows no indication of pits formed. When compared with Zn-7Ti-0.3V-S coating, few voids caused by NaCl ion were seen within the interface.

The reason for this behavior is not strange in that nonuniform distribution of composite on based metal could form agglomeration rather than strengthened bond and hence possibly affect the microstructure properties that are expected to provide strict barrier over corrosive ions. Another point to this unresilient characteristic that is in line with the work of Popoola et al.¹⁵ is the incompatibility of the composite alloy on the substrate that might result into interactive stress,

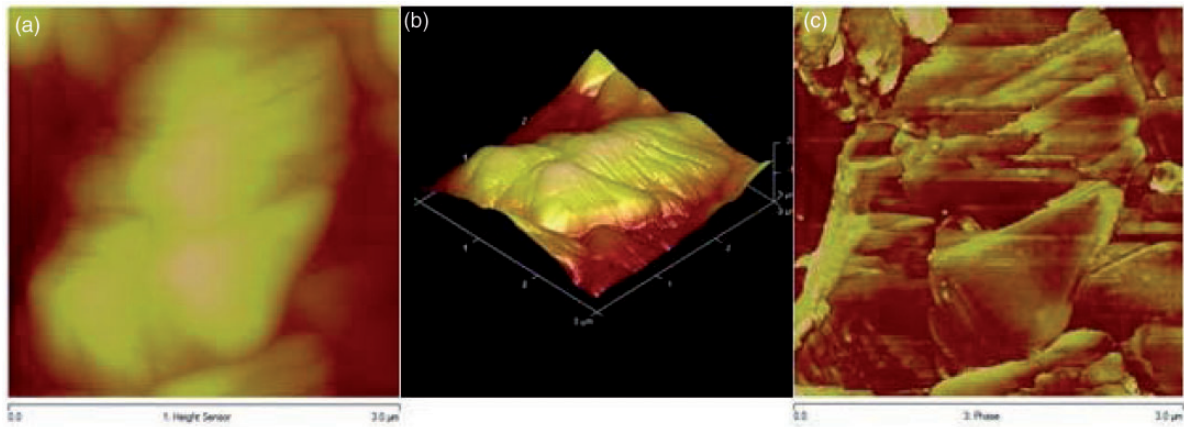


Figure 17. AFM images of the Zn-13 TiO_2 after corrosion. AFM: atomic force microscope.

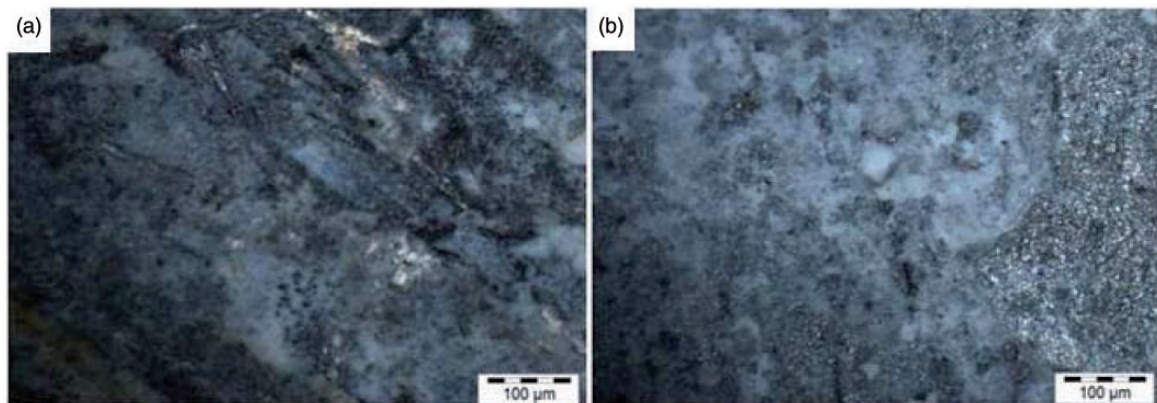


Figure 18. Micrograph of Zn- TiO_2 sulfate coatings: (a) Zn-7Ti-0.3V-S and (b) Zn-13Ti-0.3V-S.

which may then remarkably assist the process of corrosion.

Conclusions

From the results and discussion, the following conclusions can be drawn:

- The co-deposition of Zn-Ti exhibited anomalous type composite coating phenomena. Bright and compactable surfaces were produced from bath containing Zn-13Ti-0.3 V-S.
- The produced composites have shown improved mechanical properties as compared with the uncoated steel, although there was slight decrease in the adhesion of the composite coatings fabricated with 7 g wt%.
- The coefficient of friction versus time curve and sliding speed characteristics were lower for the composite produced coatings as against the as-received working sample. The wear resistance was increased by 98% as a result of an excellent surface modification.
- The addition of the TiO₂ composite particles to Zn⁺ does alter the hardness sequence as it relates to its precipitation and structural modification. The HVN of the mild steel increased greatly due to the presence of Ti particle from 34 HVN for the substrate to 154.5 HVN for Zn-13Ti-0.3 V-S composite coating.
- The increase in corrosion resistance of composite coated alloys is not due to the formation of zinc phase alone but also because of the incorporated composite of titanium, which results in the formation of solid Zn₂Ti₃ phase. This phase is significant for new crystal orientation and resistance of corrosion.

Funding

The authors thank the National Research Foundation for providing financial support and the Surface Engineering Research Centre, Tshwane University of Technology, Pretoria, South Africa, for providing equipments for conducting this study.

Conflict of interest

None declared.

References

1. Fayomi OSI and Popoola API. Chemical interaction, interfacial effect and the microstructural characterization of the induced zinc-aluminum-*Solanum tuberosum* in chloride solution on mild steel. *Res Chem Intermed* 2013; 39(64): 1313–1354.
2. Popoola API and Fayomi OS. Performance evaluation of zinc deposited mild steel in chloride medium. *Int J Electrochem Sci* 2011; 3(6): 3254–3263.
3. Praveen BM and Venkatesha TV. Electro deposition and properties of Zn-nanosized TiO₂ composite coatings. *Appl Surf Sci* 2008; 25(4): 2418–2424.
4. Sancakoglu O, Culha O, Toparli M, et al. Co-deposited Zn-submicron sized Al₂O₃ composite coatings: production, characterization and micromechanical properties. *J Mater Des* 2011; 32(9): 4054–4061.
5. Fustes J, Gomes A and da Silva Pereira MI. Electro deposition of Zn-TiO₂ nanocomposite films—effect of bath composition. *J Solid State Electrochem* 2008; 8(121): 1435–1443.
6. Wang TG, Jeong D, Liu Y, et al. Study on nanocrystalline Cr₂O₃ films deposited by arc ion plating: II. Mechanical and tribological properties. *J Surf Coat Tech* 2012; 7(206): 2638–2644.
7. Shibli SMA, Chacko F and Divya C. Al₂O₃-ZrO₂ mixed oxide composite incorporated aluminium rich zinc coatings for high wear resistance. *J Corr Sci* 2010; 9(52): 518–525.
8. Gomes A, Frade T and Nogueira ID. Morphological characterization of Zn-based nanostructured thin films. In: *Current microscopy contributions to advances in science and technology* (ed Méndez-Vilas A), vol. 2, 2012; 2(11): 1146–1153.
9. Aigbodion VS and Hassan SB. Experimental correlations between wear rate and wear parameter of Al-Cu-Mg/bagasse ash particulate composite. *Mater Des* 2009; 6(217): 2177–2180.
10. Mo JL, Zhu MH, Lei B, et al. Comparison of tribological behavior of AlCrN and TiAlN coatings-deposition by physical vapor deposition. *Wear* 2007; 5(263): 1423–1429.
11. Popoola API, Fayomi OSI and Popoola OM. Electrochemical and mechanical properties of mild steel electroplated with Zn-Al. *Int J Electrochem Sci* 2012; 7(8): 4898–4917.
12. Frade T, Bouzon Z, Gomes A, et al. Pulsed-reverse current electrodeposition of Zn and Zn-TiO₂ nanocomposite films. *Surf Coat Tech* 2010; 9(204): 3592–3598.
13. Abdel A, Barakat MA and Mohamed RM. Electroplated Zn-TiO₂-ZnO nanocomposite coating films for photocatalytic degradation of 2-chlorophenol. *Appl Surf Sci* 2008; 7(254): 4577–4583.
14. Fayomi OSI, Abdulwahab M and Popoola API. Properties evaluation of ternary surfactant-induced Zn-Ni-Al₂O₃ films on mild steel by electrolytic chemical deposition. *J Ovonic Res* 2013; (9): 123–132.
15. Popoola API, Fayomi OSI and Popoola OM. Comparative studies of microstructural, tribological and corrosion properties of plated Zn and Zn-alloy coatings. *Int J Electrochem Sci* 2012; 7(9): 4860–4870.
16. Gençağa P, Temel SS, Tevfik K, et al. Dry sliding friction and wear properties of zinc-based alloys. *Wear* 2002; 8(94): 901–906.
17. Yu SR, Liu Y, Li W, et al. The running-in tribological behavior of nano-SiO₂/Ni composite coatings. *Composites Part B: Eng* 2012; 3(43): 1070–1076.

18. Prasad BK. Effect of partially substituting copper by silicon on the physical, mechanical, and wear properties of a Zn-37.5% Al-based alloy. *Mater Charact* 2000; 44(3): 301–308.
19. Rahman MJ, Sen SR, Moniruzzaman M, et al. Morphology and properties of electrodeposited Zn-Ni alloy coatings on mild steel. *J Mech Eng* 2009; 10(40): 9–12.
20. Zhu X, Cai C, Zheng G, et al. Electrodeposition and corrosion behaviour of nanostructured Ni-Tin composite films. *Tran Non-Ferr Metals Soc China* 2011; 21(8): 2216–2224.
21. Su YL and Kao WH. Tribology tribological behavior and wear mechanism of MoS₂-Cr coatings sliding against various counterbody. *Tribolo Int* 2003; 36(12): 11–23.